CALCULATION OF AERODYNAMIC COEFFICIENTS OF MISSILE LIKE GEOMETRIES BY VISCOUS/INVISCID COUPLING

Önen, C[*],
TÜBİTAK-SAGE,
P.K.16, 06261, Mamak, Ankara, TURKEY

Yavuz, İ[**], *Kavsaoğlu, M.Ş.*[***]
Middle East Technical University,
06531, Ankara, TURKEY

Flow around aerospace vehicles and missiles can be analyzed with both inviscid and viscous numerical codes. These codes should have the capability of the computation of aerodynamic characteristics of complex configurations at the subsonic, transonic and supersonic Mach number ranges. However, there are some limitations and drawbacks of these methods. Coupling of inviscid and viscous codes can overcome these drawbacks and limitations. A similar method was applied in this study. An inviscid three dimensional panel code, NLRAERO was coupled with a viscous three dimensional boundary layer code, BL3D. This coupling procedure was applied on a missile with wrap around fins. Total drag coefficient, C_D, was calculated and compared with different methods at subsonic and supersonic Mach number ranges and the results are in well agreement.

INTRODUCTION

Analysis of flow around missile like geometries can be analyzed with both inviscid and viscous numerical codes. However, each of them has several advantages and disadvantages. A numerical procedure in which inviscid and viscous codes are coupled, has the advantages of each code while the coupling procedure disables the drawbacks of these codes.

A similar study will be performed in this paper, to monitor the viscosity effects on the aerodynamic stability derivatives for missile like geometries, especially on the drag coefficient, C_D. An inviscid panel code, NLRAERO [2] is coupled with a viscous boundary layer code, BL3D [7]. Final code is tested for a missile geometry. Brief information about these numerical codes and about the coupling procedure will be given in the following paragraphs. Test cases and results will be explained in the final part of the paper.

INVISCID PANEL CODE, NLRAERO

General Features

Design and analysis methods of aerospace vehicles and missiles require the computation of the aerodynamic characteristics of complex configurations at the subsonic, transonic and supersonic Mach number ranges.

Panel methods have proven to serve the purpose of analyzing the aerodynamics of the configurations quite adequately for subsonic and supersonic flows. This in spite of their inherent limitations requiring bodies to be slender, wing, tail and canard surfaces to be thin and at small angle of attack and side slip. The linearized potential flow model is not applicable for transonic flows and supersonic flows with strong shock waves. Another restriction with the linear panel methods is, the flow has to be attached to the surface of the configuration. This means that separated and viscous flows can not be treated with panel methods.

For computational analysis and design studies, a new panel method was developed in the NLR laboratories of the Netherlands. This code takes the theoretical approach of reference [1] as the basis. However, this new code has some extensions and new features; more general geometry definition, new mathematical formulation of the problem, new aerodynamic influence coefficients etc. All these changes in the USSAERO resulted with a new code, NLRAERO [2]. In the following sections the mathematical formulation and the computer code will be briefly discussed.

* Research engineer also graduate student at Middle East Technical University, *METU*
** Graduate student and research assistant
*** Assoc. Prof., also consultant at *TÜBİTAK-SAGE*

Description of the Method

Governing equation for the flows over objects in which the velocity is slightly perturbed from the free stream value, i.e. $\vec{u} = \vec{U}_\infty + \vec{\nabla}\varphi$, the differential equation for the perturbation velocity φ can be linearized, resulting into the linearized potential or Prandtl-Glauert equation,

$$\beta^2 \varphi_{xx} + \varphi_{yy} + \varphi_{zz} = 0, \qquad (1)$$

where $\beta^2 = 1 - M_\infty^2$, M_∞ is free stream Mach number, $\vec{U}_\infty$ is free stream velocity vector and φ is the perturbation velocity. Equation (1) is elliptic for subsonic flows and hyperbolic for supersonic flows that bring some difficulties.

It is furthermore assumed that, the x axis is aligned with the body axis, rather than the free stream direction, figure 1. This is a valid approximation within the context of linearized potential theory provided that the angle of attack and sideslip angle are small. This provides that, the governing equation is independent of the freestream direction. This has the advantage of computation of aerodynamic characteristics of a configuration at more than one angle of attack and/or sideslip at relatively little extra expense [2].

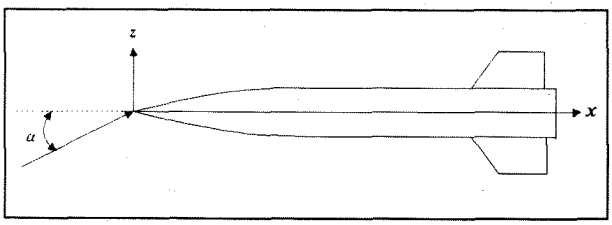

Figure 1 Coordinate System for NLRAERO.

Boundary Conditions

The boundary condition to be satisfied are;

- the flow is tangential to the surface of the configuration, in other words normal velocity is zero on the configuration;

$$\vec{u} \cdot \vec{n} = 0, \qquad (2)$$

where $\vec{n}$ is the unit normal to the surface.

- the flow is unperturbed at infinity;

$$\varphi \to 0, \qquad (3)$$

where φ is the perturbation velocity.

- Kutta condition is applied at the subsonic trailing edges of lifting components.

Linearized theory also restricts the geometry that will be solved with panel methods. Thin and mildly cambered lifting components and pointed slender nonlifting components can be solved according to this assumption. The other point with linearized theory is that, the boundary conditions and governing equations applied to the wing segment reference plane, that is a plane formed by the plane parallel to the x axis and passing through the segment leading edge, instead of the wing itself, figure 2. This is a valid approximation since, all the terms in the equation must be in the same order.

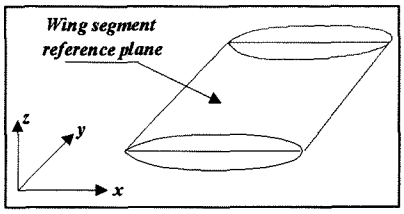

Figure 2 Wing Segment Reference Plane.

Method of Solution

Singularity distribution method is used to solve the equation (1), subject to the boundary conditions discussed in the previous paragraph. The velocity at any point $\vec{x}_0$ can be expressed as the sum of freestream velocity, velocity induced by source and doublet distributions on the wing segment reference plane(s) and a source distribution on the surface of body like components,

$$\vec{u}(\vec{x}_0) = \vec{U}_\infty + \vec{u}_q(\vec{x}_0) + \vec{u}_\mu(\vec{x}_0), \qquad (4)$$

where $\vec{u}_q(\vec{x}_0)$ is the velocity induced by the source distribution and $\vec{u}_\mu(\vec{x}_0)$ is the velocity induced by the doublet distribution.

Singularity distribution is fitted on the configuration by small four sided surfaces, that is called as "panel". Singularity distributions are located on these panels according to the type of panel. Present method utilizes the constant strength source singularities to represent the body like components. Constant strength source singularities and linearly varying doublet singularities are used for wing like components.

Geometry and Paneling Scheme

Different paneling schemes are applied for body and wing like components of the configuration. Body like components of the configuration, which may have an arbitrary cross section, are first divided into segments by transverse planes where x = constant. Body nose, central

part or tail cone may be possible examples of body segment. Then, each body segment is subdivided into rings by transverse planes at constant x values. The number of panels per ring may vary from segment to segment, figure 3.

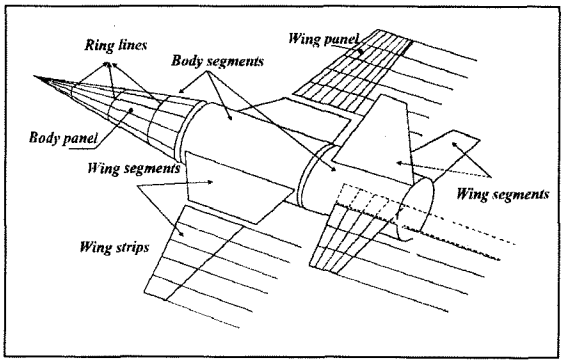

Figure 3 Paneling Scheme.

Wing like components of the configuration are first divided into segments by planes parallel to x axis. Each wing segment may be assumed as a wing segment reference plane as mentioned in the previous paragraphs. Then, each segment is subdivided into streamwise strips, that have same number of panels per strip.

Geometry and paneling input requires the specification of data per segment. Values of the panel coordinates are calculated by interpolation. Preparation of input data is hard work and it effects all the solution scheme. Insufficient or incorrect paneled configurations may result with unsatisfactory solutions, although the paneling is right.

Collocation Technique

Next step in the solution procedure is to determine that, where source and doublet singularities will be located on the panels. Collocation technique is used to determine these points. In this technique centroid of the panels are chosen as the collocation point for body like panels. The Kutta condition directly effects the place of collocation point for wing like components. In case of a subsonic trailing edge, the Kutta condition implies a zero bound vorticity at the trailing edge, while at a supersonic trailing edge a nonzero bound vorticity component is allowed. In this latter case the number of unknown parameters is increased by on, requiring one extra collocation point per strip. The application of boundary conditions, discussed in the previous paragraph, to these collocation points leads to a square system of linear equations for the unknown parameters in the body source and wing doublet distribution.

Solution Method

It is now possible to write the induced velocity as the sum of the contributions due to the source and doublet distribution,

$$\vec{u}(\vec{x}_0) = \vec{U}_\infty + \sum_{i=1}^{NB} Q_i \vec{a}_{b_i} + \sum_{i=1}^{NW} X_i \vec{a}_{w_i} + \sum_{i=1}^{NWT} q_{w_i} \vec{b}_{w_i} \qquad (5)$$

where $Q_i, i = 1, NB$ are the unknown source distribution parameters on the body like components, $X_i, i = 1, NW$ are the unknown doublet distribution on the lifting components and $q_{w_i}, i = 1, NWT$ are the known source distribution parameters on the lifting values, that are determined by using the boundary conditions. The terms, $\vec{a}_b, \vec{a}_w$ and $\vec{b}_w$, are the aerodynamic influence coefficients, that depend on geometry conditions. Hence, symmetry properties must be used to reduce the operation number in calculations

Resulting system is a set of linear equations, that have $NB + NW$ equations and $NB + NW$ unknowns. This system of equations is solved by a block Jacobi iteration method using the residual correction. Iteration number is about 20-30 for subsonic Mach numbers, while in supersonic Mach numbers it is less than 20.

Pressure distribution, forces and moments

The final step in the solution procedure is determination of pressure. Different expressions are used for body and wing like components. Bernoulli's isentropic expression is used for body like components,

$$p = p_\infty + \frac{\rho_\infty U_\infty^2}{\gamma M_\infty^2}\left[\left\{1 - \frac{\gamma - 1}{2} M_\infty^2 \left(\frac{|\vec{u}|^2}{U_\infty^2} - 1\right)\right\}^{\frac{\gamma}{\gamma - 1}} - 1\right], \qquad (6)$$

where p_∞ is freestream pressure, ρ_∞ is freestream density and γ is the ratio of specific heats. Expansion of equation (6) for small perturbations leads to the linear expression for the pressure on wing like components,

$$p = p_\infty - \rho_\infty U_\infty \frac{\partial \varphi}{\partial x}. \qquad (7)$$

Then the aerodynamic forces can be found using,

$$\vec{F} = \frac{1}{2}\rho_\infty U_\infty^2 \iint_{S_{wing}} c_p \vec{n}_w dS - \iint_{S_{body}} c_p \vec{n}_b dS \qquad (8)$$

and the moments can be found by,

$$\vec{M} = -\frac{1}{2}\rho_\infty U_\infty^2 \iint_{S_{wing}} c_p \vec{r} \times \vec{n}_w dS - \iint_{S_{body}} c_p \vec{r} \times \vec{n}_b dS \qquad (9)$$

where c_p is pressure coefficient, $\vec{r}$ is the vector pointing from the moment reference point to the any point on the configuration and $\vec{n}_b, \vec{n}_w$ are the unit normal vectors to body and wing surfaces respectively

VISCOUS BOUNDARY LAYER CODE, BL3D

Boundary layer methods are in advantage in cost efficiency, but have a limited predictive capability against the Navier -Stokes solution methods. However, as its speed is considered, they are essential in any typical design environment. There exist many different methods dealing with three-dimensional boundary layers, which use either the global (integral methods) or local (finite-difference methods) equation set. Some of these are the ones regarded by Bradshaw [3], Smith [4], Michel et al [5], Cebeci and Chang [6], and Van Dalsem and Steger [7].

In the present study the boundary layer solution code BL3D is applied to the solution of the studied cases, where the surface pressure required is provided by NLRAERO. The finite-difference solution algorithm [7] is used, and the integration of the boundary layer equations are carried out using the Van Dalsem-Steger [7] finite-difference time-relaxation algorithm. As the turbulence model is considered, the Cebeci-Smith Method is applied in this study.

Governing Equations

For the Boundary Layer Equations a simple coordinate transformation from the Cartesian coordinates (x,y,z) to general curvilinear coordinates $\xi(x,z)$, $\eta(x,y,z)$ and $\zeta(x,z)$ is used. The surface curvature is neglected in the unsteady compressible boundary-layer equations, so the three dimensional equations for a perfect gas can be written as;

x-momentum equation,

$$\rho u_t + \rho\left(U u_\xi + V u_\eta + W u_\zeta\right) = -\beta\left(p_\xi \xi_x + p_\zeta \zeta_x\right) + \left(\mu u_\eta \eta_y\right)_\eta \eta_y, \qquad (10)$$

z-momentum equation,

$$\rho w_t + \rho\left(U w_\xi + V w_\eta + W w_\zeta\right) = -\beta\left(p_\xi \xi_z + p_\zeta \zeta_z\right) + \left(\mu w_\eta \eta_y\right)_\eta \eta_y, \qquad (11)$$

perfect gas relation,

$$p = \rho T, \qquad (12)$$

energy equation (H = total enthalpy),

$$H_t + \rho\left(U H_\xi + V H_\eta + W H_\zeta\right) = \left[\frac{\mu}{\mathrm{Pr}}\left\{H_\eta \eta_y + \frac{\mathrm{Pr}-1}{2}\left(u^2 + w^2\right)_\eta \eta_y\right\}\right]_\eta \eta_y, \qquad (13)$$

and continuity equation,

$$\rho_t + (\rho u)_\xi \xi_x + (\rho u)_\eta \eta_x + (\rho u)_\zeta \zeta_x + (\rho v)_\eta \eta_y + (\rho w)_\xi \xi_z + (\rho w)_\eta \eta_z + (\rho w)_\zeta \zeta_z = 0. \qquad (14)$$

In these equations U, V and W are unscaled contravariant velocities,

$$\begin{bmatrix} U \\ V \\ W \end{bmatrix} = \begin{bmatrix} \xi_t + \xi_x u + \xi_z w \\ \eta_t + \eta_x u + \eta_y v + \eta_z w \\ \zeta_t + \zeta_x u + \zeta_z w \end{bmatrix}, \qquad (15)$$

and

$$\beta = \left(\frac{p}{\rho u^2}\right)_\infty. \qquad (16)$$

The Cartesian u and w velocities are parallel to the body, and Cartesian coordinates x and y are non-dimensionalized by the free-stream velocity and a characteristic length, respectively. Also the v and y variables are non-dimensionalized by the same values divided by $\sqrt{\mathrm{Re}_\infty}$. Density, pressure, temperature and viscosity are non-dimensionalized by their free-stream values. For turbulent flows, the molecular and eddy-viscosities are summed up to find the viscosity coefficient μ.

Numerical Algorithm

There is no need for complex space-marching patterns, since a time-like algorithm is used. Moreover the boundary layer equations are weakly coupled, as the

pressure gradient forcing terms in the momentum equations are treated as given functions. Therefore these can be solved sequentially at each time step. As a result, a semi-implicit algorithm can be used at each time or iterative step, yet only scalar-like uncoupled equations are solved. Implicit second-order accurate central-difference operators in the direction normal to the body η, and flow dependent second-order accurate operators in the other two directions ξ and ζ are used in the approximation of the spatial derivatives in the momentum and energy equations.

The time-accurate algorithm, using conventional operators in terms of the shift operator $E_\xi^{\pm 1} u_j = u_{j\pm 1}$ is written as;

$$\nabla_\xi = \left(1 - E_\xi^{-1}\right)/\Delta\xi, \tag{17}$$

$$\Delta_\xi = \left(E_\xi^{+1} - 1\right)/\Delta\xi, \tag{18}$$

$$\delta_\xi = \left(E_\xi^{+1} - E_\xi^{-1}\right)/\left(2\Delta\xi\right), \tag{19}$$

$$\bar{\delta}_\xi = \left(E_\xi^{+\frac{1}{2}} - E_\xi^{-\frac{1}{2}}\right)/\left(2\Delta\xi\right), \tag{20}$$

and the second order accurate upwind operator

$$\hat{\alpha}\hat{\delta}_\xi = \left(\frac{\alpha + |\alpha|}{2}\right)\nabla_\xi\left(\frac{3 - E_\xi^{-1}}{2}\right) + \left(\frac{\alpha - |\alpha|}{2}\right)\Delta_\xi\left(\frac{3 - E_\xi^{+1}}{2}\right), \tag{21}$$

where α is the convective coefficient.

The semi-implicit scheme

Update u at the new time step from the x-momentum equation,

$$\rho\nabla_t u^{n+1} + \rho\left(\hat{U}\hat{\delta}_\xi u^{n+1} + V\delta_\eta u^{n+1} + \hat{W}\hat{\delta}_\zeta u\right) = -\beta\left(\xi_x\delta_\xi p + \zeta_x\delta_\zeta p\right) + \eta_y\bar{\delta}_\eta\left(\mu\eta_y\bar{\delta}u^{n+1}\right), \tag{22}$$

where ∇, δ and $\bar{\delta}$ are the first-order backward-difference, second-order central-difference and second-order mid-point central-difference operators, respectively. And $\hat{U}\hat{\delta}$ denotes the second-order accurate upwind-difference operator. By inverting scalar-tridiagonal matrices in η, this system of equations can be easily solved. In the same way, w is updated from the z-momentum equation,

$$\rho\nabla_t w^{n+1} + \rho\hat{U}\hat{\delta}_\xi w^{n+1} + \rho V\delta_\eta w^{n+1} + \rho\hat{W}\hat{\delta}_\zeta w = -\beta\left(\xi_z\delta_\xi p + \zeta_z\delta_\zeta p\right) + \eta_y\bar{\delta}_\eta\left(\mu\eta_y\bar{\delta}w^{n+1}\right), \tag{23}$$

and H is updated from the energy equation,

$$\rho\nabla_t H^{n+1} + \rho\left(\hat{U}\hat{\delta}_\xi H^{n+1} + V\delta_\eta H^{n+1} + \hat{W}\hat{\delta}_\zeta H\right) = \eta_y\bar{\delta}_y\left[\frac{\mu}{\mathrm{Pr}}\left\{\eta_y\bar{\delta}_\eta H^{n+1}\right\}\right] + \eta_y\bar{\delta}_y\left[\frac{\mu}{\mathrm{Pr}}\left\{\frac{\mathrm{Pr}-1}{2}\eta_y\bar{\delta}_\eta\left(u^2 + w^2\right)^{n+1}\right\}\right], \tag{24}$$

or, a constant total enthalpy assumption, for many steady-state cases, can replace this partial-differential equation.

Then, obtain the density $\rho = p/T$ and integrate the continuity equation for v using the updated values of u, w and ρ;

$$\nabla_\eta(\rho v)^{n+1} = -\frac{1 + E_\eta^{-1}}{2}.(A + B + C)^{n+1}, \tag{25}$$

where

$$A = \xi_x\delta_\xi(\rho u) + \eta_x\delta_\eta(\rho u) + \zeta_x\delta_\zeta(\rho u), \tag{26}$$

$$B = \xi_z\delta_\xi(\rho w) + \eta_z\delta_\eta(\rho w) + \zeta_z\delta_\zeta(\rho w), \tag{27}$$

and

$$C = \nabla_t\rho. \tag{28}$$

The Turbulence Model

The Cebeci-Smith [CS] Model (1974)

The Cebeci-Smith (1974) turbulence model is a two-layer algebraic eddy-viscosity model. It uses a Prandtl-van Driest formulation for the inner and a Clauser formulation together with Klebanoff's intermittency function for the outer region.

The eddy-viscosity is described by

$$\upsilon_t = \begin{cases} \upsilon_{ti} & \text{for } y \le y^* \\ \upsilon_{to} & \text{for } y > y^* \end{cases}, \tag{29}$$

where y^* is the smallest value of y at which the eddy-viscosity values from the inner and outer region are identical.

In the inner region, the eddy-viscosity is taken as

$$\upsilon_{ti} = (D\kappa y)^2 \left[\left(\frac{\partial u}{\partial y} \right)^2 + \left(\frac{\partial w}{\partial y} \right)^2 \right]^{1/2}, \quad (30)$$

where $\partial u/\partial y$ and $\partial w/\partial y$ are the components of the velocity-gradient vector, y is the normal distance and $\kappa = 0.41$ is the Karman's constant. The near-wall damping D is given as;

$$D = 1 - e^{-y^+/A^+}, \quad (31)$$

where $A^+ = 26$ and y^+ is given by

$$y^+ = \frac{\sqrt{\rho_w |\tau_w|}\, y}{\mu_w}. \quad (32)$$

The subscript w denotes values to be taken at walls.

For the outer layer, Clauser's formulation together with Klebanoff's intermittency function is used

$$\upsilon_{to} = k q_e \delta_i^* F_{Kleb}, \quad (33)$$

where δ_i^* is the incompressible (total) boundary layer displacement thickness

$$\delta_i^* = \int_0^\delta \left(1 - \frac{q}{q_e} \right) dy, \quad (34)$$

δ being the boundary layer thickness and $q = \left(u^2 + w^2 \right)^{1/2}$ is the magnitude of the mean velocity. Although varying slightly in the low-momentum-Reynolds-number range, the Clauser parameter k is generally taken to be a constant, $k = 0.0168$, and the Klebanoff's intermittency function is,

$$F_{Kleb} = \frac{1}{1 + 5.5 \left(y/\delta \right)^6}, \quad (35)$$

Finally, the eddy-viscosity distribution is found from

$$\upsilon_t = \min\left(\upsilon_{ti}, \upsilon_{to} \right). \quad (36)$$

COUPLING PROCEDURE

Direct way of coupling procedure is chosen for this study. Pressure values obtained from the NLRAERO are input to the BL3D by some modifications. Where the body and the fins are all separated. This means that the BL3D code must run five times to solve a missile like geometry with four fins. Boundary layer thickness and skin friction values are calculated in this viscous code, according to the pressure values. Skin friction values are checked with the experimental data in that step. If the values are accurate enough the procedure ends and viscous drag coefficient is calculated by integrating the skin friction values over the body surface. If not, the distributions of the boundary layer thickness are added to the original geometry at each point. This modified geometry is the new input of the panel code NLRAERO. New values of pressure are calculated and fed back to the boundary layer code BL3D. This iterative procedure stops if the calculated values have converged or close enough to the experimental values. Addition of boundary layer thickness to the original geometry was not performed in this study. Instead, only pressure values obtained from NLRAERO were fed to BL3D code and results are taken.

RESULTS

The test case is a missile geometry [8]. Geometric details of the missile can be shown in Figure 4.

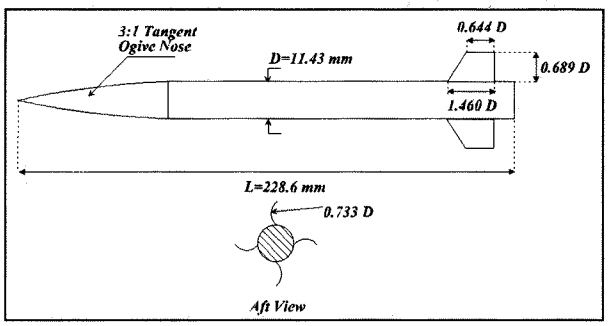

Figure 4 Geometry of the Test Case I, [8].

In order to check the results of NLRAERO for the test case, pressure distribution results for the body without the fins, was compared with an unstructured mesh based, Navier-Stokes, Euler code, NSC2KE [11]. For this case, a mesh was generated, which is given in figure 5 and 6, where L is the total body length.

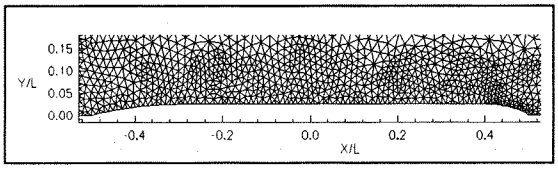

Figure 5 Enlarged View of NSC2KE Grid.

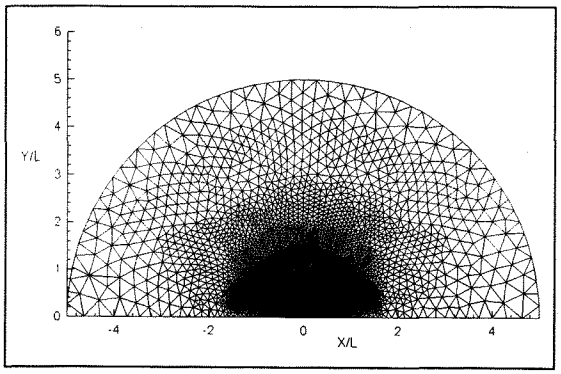

Figure 6 Grid of the Test Case for the NSC2KE Code.

The pressure values obtained with NLRAERO and NSC2KE,along the x axis of the configuration for a subsonic Mach number, $M = 0.5$, are given in figure 7, and for a supersonic Mach number, $M = 2.0$, are given in figure 8.

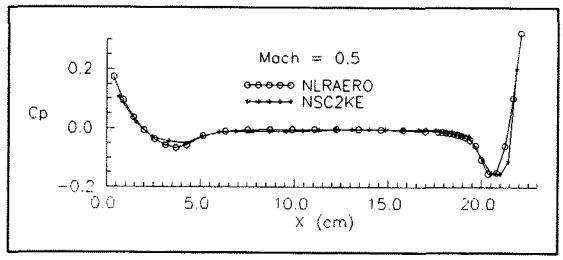

Figure 7 Body Alone Surface Pressure Values at $M = 0.5$.

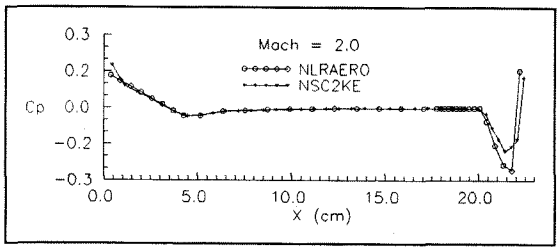

Figure 8 Body Alone Surface Pressure Values at $M = 2.0$.

It can be said that pressure values calculated by the panel code, NLRAERO are quite good in subsonic and supersonic Mach numbers. However, there is a slight difference between the values of these codes at supersonic speeds especially at the rear end of the body.

The grid produced to be used in BL3D code is shown in figure 9. Here the growth of the boundary layer is taken into account. Although, it is not a very complex grid, compared to Navier-Stokes and Euler grids, is enough to obtain good results. Figure 9 shows only the grid at one angle around the body in the normal direction to the surface, where S designates the surface distance along the body. A similar grid is produced for the fins, that was placed at the clustered region at the back of the grid.

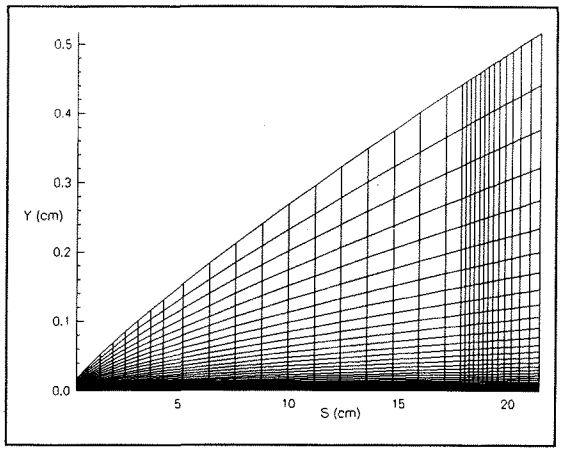

Figure 9 Boundary Layer Grid of the Test Case.

Then the pressure distribution is taken as an input of the BL3D code and boundary layer parameters are calculated. Skin friction coefficient, C_f, distribution for two Mach numbers, $M = 0.5$ and $M = 2.0$ are shown in figure 10.

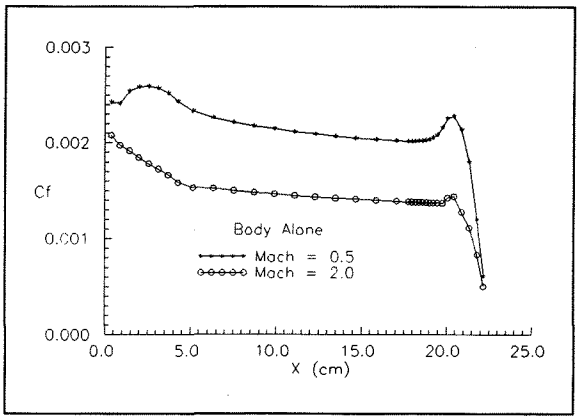

Figure 10 C_f Distribution for the Body Alone.

The BL3D code is only able to calculate the viscous drag by integrating the skin friction drag along the body. Therefore, in order to find the total drag, the pressure or wave and base drag values are taken from the MISSILE DATCOM [9].

A comparison of the viscous drag variation with the Mach number, calculated by MISSILE DATCOM and BL3D for the body alone configuration, is shown in figure 11. It can be easily said that, viscous drag coefficients calculated with BL3D are in well agreement with the MISSILE DATCOM results.

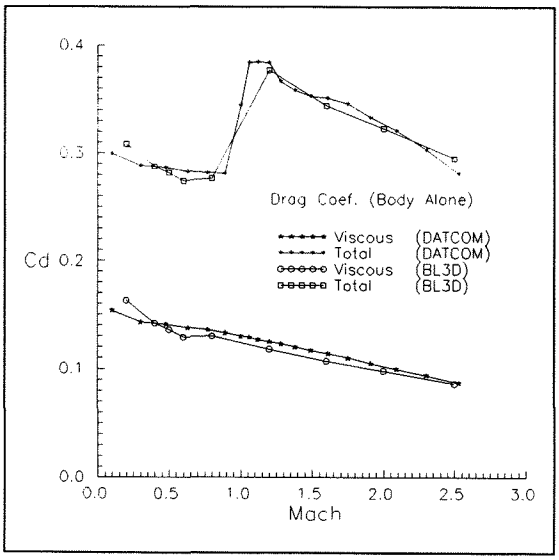

Figure 11 Body Alone Viscous and Total Drag Coefficients.

For the whole missile, i.e. body and fins, variation of the total drag coefficient, C_D, at zero angle of attack, with the Mach number, was obtained from five different sources. Which were the MISSILE DATCOM code, the vortex lattice panel code, VORLAX [10], and the EAGLE code obtained from reference [8], and the result of this study in which the 3-D panel code NLRAERO are coupled with the 3-D boundary layer code, BL3D. Result of the NLRAERO code alone is also shown in figure 12 to give an idea about the pressure drag.

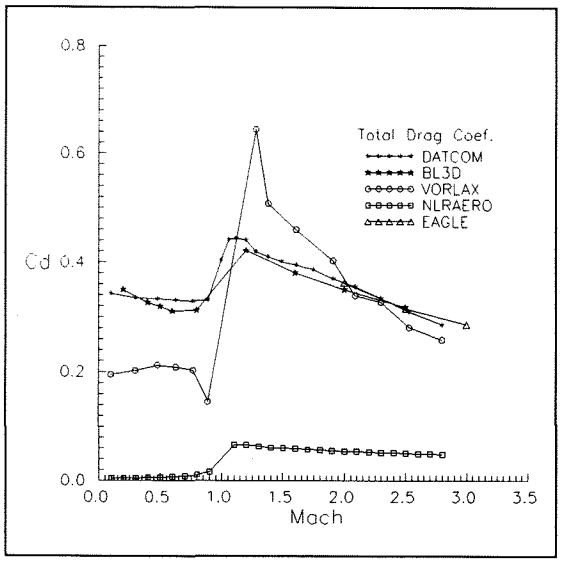

Figure 12 Drag Coefficient of Test Case I.

It can be said that calculations of BL3D and NLRAERO are in agreement with the results of MISSILE DATCOM. This indicates that, coupling procedure is successful and results are very accurate when compared with the experimental values. The drag coefficient calculated with NLRAERO only is very small although the general trend is similar to the total drag coefficient. However, by coupling procedure results are improved, that is the aim of this study.

CONCLUSIONS

An inviscid panel code, NLRAERO was coupled with a viscous boundary layer code BL3D. Skin friction drag calculated with BL3D and total drag was compared with the other numerical results. A wrap around finned missile geometry was chosen as the test case and the flow around it was solved at zero angle of attack, $\alpha = 0°$. Results of this case were in well agreement when compared with the results of other codes.

Another case, the flow around the prolate spheroid at $\alpha = 10°$ was attempted to be solved. However, the BL3D code was not able to solve the flow in the pressure specified mode, since the flow separates on the body. To overcome this difficulty the skin friction specified case must be solved, which was not in the scope of this study. Thus, there is a difficulty in analyzing the separated flows with inviscid viscous coupling. But, if there is no separation, the results are very well when compared to other methods.

REFERENCES

1. Woodward, F.A., "*USSAERO, An improved method for the aerodynamic analysis of wing-body-tail configurations in subsonic and supersonic flow*", NASA CR-2228, 1973.

2. Hoeijmakers, H.W.M., "*A panel method for the determination of the aerodynamic characteristics of complex configurations in linearized subsonic and supersonic*", NLR TR 80124 U, 1980.

3. Bradshaw, P., "*Calculation of three-dimensional turbulent boundary layers*", J. Fluid Mech. 46, 417, 1971.

4. Smith, P. D., "*An integral prediction method for three-dimensional compressible turbulent boundary layers*", Report ARC TR 72228, 1973.

5. Michel R., Cousteix J., and Quemard C., "*Methode practique de prevision des couches limites turbulentes bi- et tri-dimensionelles*", Rech. Aerosp. No. 1, 1972.

6. Cebeci, T. and Chang, K. C., "*On the turbulence modeling requirements of three-dimensional flows*", Recent Contributions to Fluid Mechanics, (Edited by W. Haase), Springer, New York (1982).

7. Van Dalsem, W. R. and Steger, J. L., "*Efficient simulation of separated three-dimensional viscous flows using the boundary layer equations*", AIAA J. 25, 395, 1987.

8. Vitale, L.R., Abate, G.L., Winchenbach, G.L., "*Aerodynamic Test and Analysis of a Missile Configuration with Curved Fins*", AIAA-92-4495-CP, 1992.

9. Vukelich, S.R., "*Development and Feasibility of MISSILE DATCOM*", AFWAL-TR-81-3139, 1981.

10. Miranda, L.R., Elliot, R.D., Baker, W.M., "*A Generalized Vortex Lattice Method for Subsonic and Supersonic Flow Applications*", NASA-CR-2865, 1973.

11. Bijan, M., "*Fluid Dynamics Computation with NSC2KE, An User-Guide Release 1.0*", Institute National De Recherche en Informatique et en Automatique, INRIA Report No: RT-0164, 1994.